Hydronamic micro-encapsulation of aqueous fluids and cells via 'on the fly' photopolymerization

Article *in* Journal of Micromechanics and Microengineering · February 2006

DOI: 10.1088/0960-1317/16/2/013

INSTITUTE OF PHYSICS PUBLISHING JOURNAL OF MICROMECHANICS AND MICROENGINEERING

J. Micromech. Microeng. **16** (2006) 285–291 doi:10.1088/0960-1317/16/2/013

Hydrodynamic micro-encapsulation of aqueous fluids and cells via '*on the fly*' photopolymerization

Hyun-Jik Oh[1], **So-Hyun Kim**[1], **Ju-Yeoul Baek**[1], **Gi-Hun Seong**[2] **and Sang-Hoon Lee**[1]

[1] Department of Biomedical Engineering, Dankook University, San 29, Anseodong Cheonan, 330-714, Korea
[2] Department of Chemistry, Hanyang University, Sa-1 dong 1271, Ansan 425-791, Korea

E-mail: dbiomed@dankook.ac.kr

Received 14 July 2005, in final form 7 November 2005
Published 9 January 2006
Online at stacks.iop.org/JMM/16/285

Abstract
We report a new technique that, in contrast to conventional methods, uses a microfluidic platform for the fabrication of polymeric microcapsules that can contain sensitive biological materials. This encapsulation process is carried out through the use of hydrodynamic phenomena (e.g., multiphase laminar flow), and 'on the fly' photopolymerization. Our method allows for the generation of microcapsules whose size can be controlled by a regulation of flow rates, and the polymerized capsule can protect fragile materials, such as cells, DNA and enzymes from harsh environments. The proposed approach is extended to the fabrication of a microcontainer that can handle small volumes of liquid. The flexibility of the method across different materials and scales is a key advantage over many existing methods.

M This article features online multimedia enhancements

(Some figures in this article are in colour only in the electronic version)

1. Introduction

Recent progress in chemical, biological and clinical technology has resulted in many therapeutic materials such as chemical drugs, cells and recombinant proteins in large quantities. However, the delivery of these materials has been limited to oral and parenteral administration. Also important to the maximization of the therapeutic effect during drug delivery are (1) the delivery of these materials to specific areas inside the body, (2) the protection of these materials against harsh conditions, (3) the maintenance of these materials' functional integrity and (4) the prevention of toxic drugs' severe side effects. One way to realize such delivery is to form the micrometer-sized capsules from the bulk components so that the capsules have a controllable and adjustable coating thickness, and diverse fabrication methods have been reported that make use of emulsion technology, electrohydrodynamic force, layer-by-layer deposition of polyelectrolyte multilayers and so forth [1–8]. They are very advantageous methods for the realization of micro-encapsulation but still have limitations related to (1) the ability to produce a uniform-sized microcapsule, (2) the stabilization of sensitive materials inside microcapsules and (3) the expensive and time consuming production process. Another method overcoming these limitations is the production of polymeric microcapsules that makes use of a microfluidic platform. Recently, microfluidic devices have been widely used for the production of liquid micro-vesicles [9–13], and for the encapsulation of small volumes of liquid (shells are not solidified) [14, 15]. The method based on the microfluidic platform has many advantages, such as (1) the production of microcapsules that have uniform sizes and (2) overall simplicity and cost effectiveness in fabrication. However, most of such encapsulation methods are limited to the production of capsules that have un-solidified shells. We and other researchers have employed such microfluidic devices for a continuous mass production of curved polymer microstructures (such as fibers, tubes and

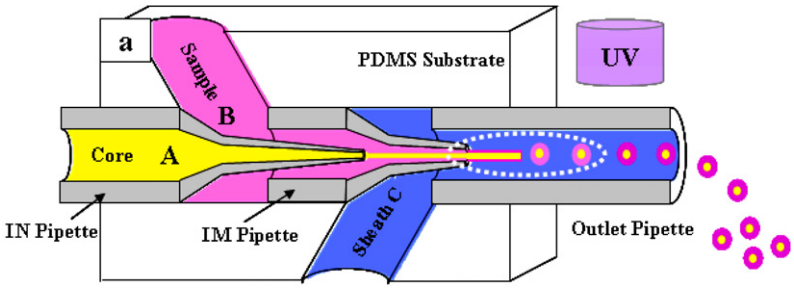

Figure 1. Schematic illustration of both the microcapsule-fabrication apparatus (MCFA) and the production microcapsules via '*on the fly*' photopolymerization.

spheres) that is based on micro scale phenomena (e.g., laminar flow) and via '*on the fly*' solidification [16–18]. Similarly, the generation of solidified microcapsules that is based on the microfluidic platform and *in situ* polymerization technology has been reported [19–21]. Despite their many advantages over conventional encapsulation methods, the above methods encounter two limitations in relation to the loading of sensitive materials into the capsule: (1) the polymerization time (UV exposure time) is long (more than a few seconds), and it may affect the sensitive material loaded inside the capsule, and (2) these methods employ mineral or silicon oil as a sheath or core fluid to generate the microcapsule through the use of microfluidic platform (this is one of the shortcomings that characterizes the loading of sensitive materials). In this paper, we report a method that is for the fabrication of polymeric microcapsules and that overcomes these limits. We minimized the polymerization time (within 200 ms) by using a fast polymerizable solution and by radiating the UV light around the outlet pipette (i.e., the UV light is radiated onto the liquid microcapsule uniformly from all directions because the reflected light is radiated onto the liquid capsule from the opposite direction of UV source). In addition, we employed aqueous solutions instead of oil, and this is one of the important advantages to our loading of sensitive materials into the capsule. To prove that the sensitive materials are loaded well and are not damaged during the fabrication process, we encapsulated the yeast cells with culturing media inside the microcapsules, stored them for 2 days and checked their viability. As another application of our method, we showed the feasibility of bundled encapsulation by the change of flow rate, and this technique will be applied as a novel tool for the storing, handling and arrayed assay of such small volumes.

2. Methods and experiments

2.1. Structure and construction of apparatus for microcapsule production

To produce microcapsules, we employed hydrodynamic phenomena (laminar flow in a micro scale channel) and the schematic of the microcapsule-fabrication apparatus (MCFA) is demonstrated in figure 1. We employed two kinds of pulled pipettes—the inlet pipette (IN-pipette) and the intermediate pipette (IM-pipette)—and one normal (non-pulled) outlet pipette (O-pipette) to make the focused flow and the outlet flow. We constructed the apparatus by combining

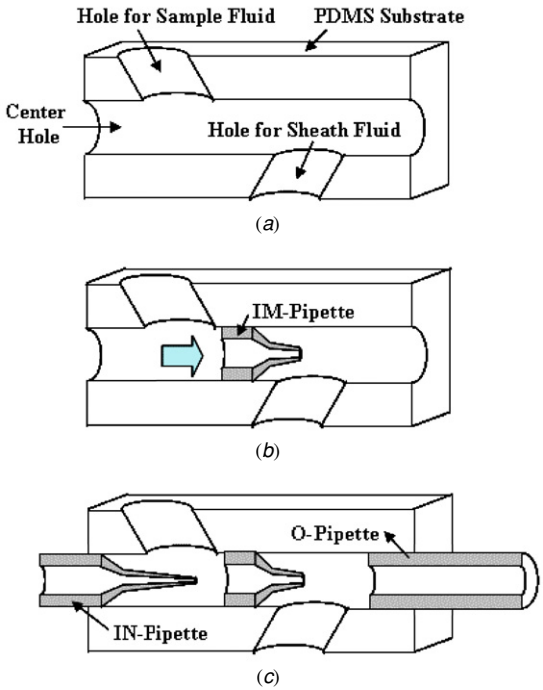

Figure 2. Cross-sectional diagram of (*a*) prepared PDMS substrate (holes for sample and sheath fluids are punctured with a 12-gauge needle). (*b*) Insertion and bonding of IM-pipette (for better insertion, methanol was employed as a lubricant). (*c*) Insertion and bonding of IN- and O-pipettes.

three kinds of pipettes and the PDMS substrate with a pre-punctured center hole. The fabrication method of the PDMS substrate is described in our previous report [16]. To make the pulled micropipette, we employed a glass micropipette (Aluminosilicate glass/1714, Corning) whose length was 4 cm, and whose inner and outer diameters were 0.5 mm and 1 mm respectively. Before inserting the micropipette into the center hole of PDMS substrate, we cored out the holes for the sample and the sheath fluids using a 12-gauge needle, as illustrated in figure 2(*a*). Onto both the prepared PDMS substrate and the IM-pipette, the oxygen plasma was exposed for 2 min. We introduced the IM-pipette through the center hole by using methanol as a lubricant, and we bonded the IM-pipette onto the inner surface of center hole by curing for 4 h at 80 °C, as shown in figure 2(*b*). The IN-pipette and the O-pipette were exposed to the oxygen plasma, introduced into both ends of the center hole and bonded via the curing for 4 h at 80 °C, as shown in figure 2(*c*). We shielded the

Table 1. Compound and concentration of sample and sheath fluid.

Solution no.	Compound and concentration
Solution 1	4-HBA solution + PI (3.415 wt%)
Solution 2	Solution 1 + AA (13.842 wt%) + EGDMA (0.962 wt%)
Solution 3	PVA (25 Vol%) + DI (75 Vol%) water

4-HBA solution: 4-HBA (4-hydroxy butyl acrylate), PI (photoinitiator): 2,2-dimethoxy-2-phenylacetophenone (DMPA), cross-linker: ethylene glycol dimethacrylate (EGDMA), AA: acrylic acid, PVA: polyvinylalcohol, DI: deionized.

fabricated apparatus with aluminum foil, so that the UV light is radiated only onto the outlet pipette.

2.2. Encapsulation principle

Using syringe pumps, we introduced into the three inlets, respectively, the core fluid, the photopolymerizable sample fluid and the sheath fluid. We encapsulated two kinds of core materials, such as dyed water (solution 3 + red dye) and cells (yeast cell + culture media), and the compound and the concentration of sample monomers (solution 1, viscosity: 9.73 cP) and sheath fluid (solution 3, viscosity: 9.01 cP) are summarized in table 1. The core and the sample fluid were introduced into each inlet port and traveled through the IM-pipette forming the coaxial geometry, and they were hydrodynamically focused at the tip of the IM-pipette. The focused and extruded coaxial jet flow was extended into the outlet pipette and subsequently split into segments maintaining its integrity. The mechanism of droplet formation from a cylindrical jet flow can be explained through the Rayleigh–Plateau hydrodynamic instability, and many theoretical and experimental papers that predict the jet length and droplet size have been published [22–29]. In the device that has the similar geometry with our MCFA, two drop-formation mechanisms are defined: dripping and jetting [30]. Utada *et al* reported that the transition from dripping to jetting occurs when an effective capillary number ($C_a = \eta_{sh} v/\gamma$, where η_{sh} is the viscosity of sheath fluid, v the downstream velocity of the inner fluid, γ the interfacial tension) is over 1 [20]. We have generated the microcapsules inside the MCFA via the jetting regime, and the break-up of a liquid jet formed by a coaxial thread, which consists of core fluid (dyed water) and a polymerizable sample fluid, occurred. Finally, these break-ups turn into the spherical microcapsules owing to the surface tension, and they move into the downstream channel (O-pipette). With regard to the sheath fluid, we have here utilized solution 3, which allows for water solubility. Therefore, the remnant of this solution on the surface of solidified microcapsule can be easily removed with water.

2.3. 'On the fly' solidification of capsules' shell

To solidify the sample fluid as it moved through the outlet, we exposed the transition or capsulated flow to ultraviolet (UV) radiation (365 nm, Novacure® 2100, EXFO Photonic Solution Inc) that had an intensity of 300 mW cm^{-2}. The UV light rapidly polymerized the traveling microcapsules (a rough estimate is that they were polymerized within 200 ms).

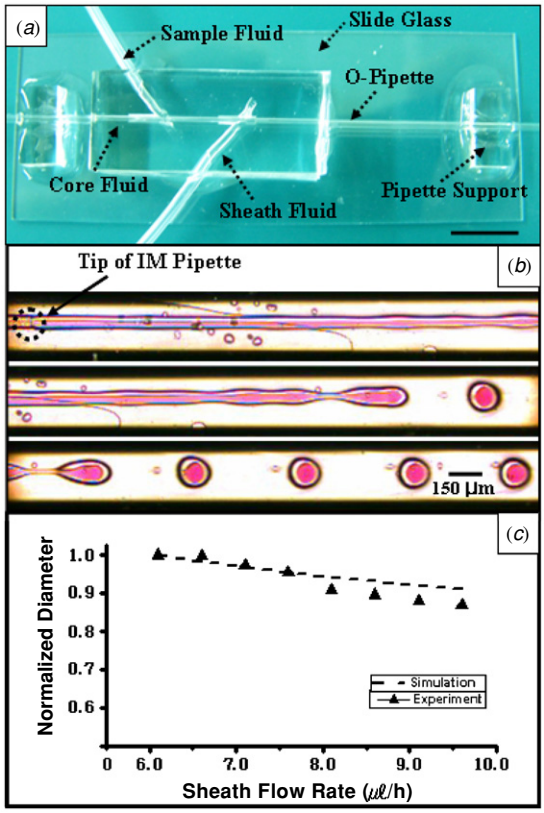

Figure 3. (*a*) Photograph of the MCFA. The MCFA is ready to produce the microcapsules continuously. (Scale bar is 1 cm.) (*b*) Optical microscopy images of the break-up of a liquid jet formed by a coaxial stream of core fluid (dyed water with red color) and polymerizable sample fluid. The resulting spherical microcapsules flow into the downstream channel: $Q_{co} = 1.25\ \mu l\ min^{-1}$, $Q_{sa} = 7.0\ \mu l\ min^{-1}$, $Q_{sh} = 133\ \mu l\ min^{-1}$. (*c*) The experimental and the calculated diameters (both values are normalized) of microcapsules according to the change of sheath flow rate: $Q_{co} = 1.50\ \mu l\ min^{-1}$, $Q_{sa} = 7.0\ \mu l\ min^{-1}$.

3. Results and discussion

3.1. Solidified diverse microcapsule

The MCFA was fabricated, and figure 3(*a*) illustrates the MCFA ready to produce the microcapsules continuously. Our device has many advantages: (1) it is very easy and simple to fabricate and (2) alignment of the core, sample and sheath flow is easy. As illustrated in this figure, the UV light is radiated onto the outlet pipette directly, and the reflected light from the bottom slide glass radiates onto the opposite side of the pipette. We guess that this structure helps to radiate light onto the surface of moving liquid-capsules uniformly, and such radiation may speed up the polymerization process.

We introduced the core, sample and sheath fluid by using syringe pumps, and figure 3(*b*) illustrates the optical microscopy images of the break-up of a liquid jet formed by both a coaxial stream of core fluid (dyed with red color) and polymerizable sample fluid, and the resulting spherical microcapsules flowed into the downstream channel. According to this figure, which was taken on a high-speed camera (APX-RS250KC, Photron) at the rate of 250 frames s^{-1}, the droplet formation that uses no oil is

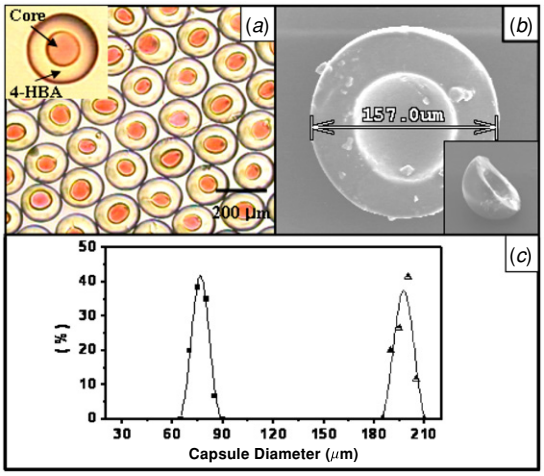

Figure 4. (*a*) Polymerized microcapsules and zoomed micrograph of a single microcapsule. The 4-HBA region is solidified, and the core region is in a liquid state: $Q_{co} = 1.22\ \mu l\ min^{-1}$, $Q_{sa} = 7.1\ \mu l\ min^{-1}$, $Q_{sh} = 133\ \mu l\ min^{-1}$. (*b*) Cross-sectional scanning electron microscopy (SEM(S-4300, Hitachi)) image of solidified microcapsule (inset is the side view). (*c*) Distribution of inner and outer diameters of produced microcapsules: $Q_{co} = 1.10\ \mu l\ min^{-1}$, $Q_{sa} = 7.1\ \mu l\ min^{-1}$, $Q_{sh} = 125\ \mu l\ min^{-1}$.

feasible. This is very important from the practical aspect. If we employ oil as a sheath fluid, the remnant mineral oils on the surface of the capsule should be removed for the biological or medical applications. However, the complete removal is not easy as the polymerized hydrogel shell is weak, and the trial to clean the surface may result in damage to the sensitive materials inside the capsule.

The inner and outer diameters of the microcapsule can be varied according to the flow rates. In a jetting regime, the drop radius is given by

$$R_{drop} = \left(\frac{15 Q_{sum}}{\pi}\frac{R_{jet}\eta_{sh}}{\gamma}\right)^{1/3} \tag{1}$$

$$\frac{Q_{sa}+Q_{co}}{Q_{sh}} = \frac{\eta_{sh}}{\eta_{sa}}\frac{\varepsilon^4}{(1-\varepsilon^2)^2} + 2\frac{\varepsilon^2}{1-\varepsilon^2} \tag{2}$$

where $\varepsilon = R_{jet}/R_{Orifice}$, $Q_{sum} : Q_{co}$ (flow rate of core fluid) + Q_{sa} (flow rate of core fluid), Q_{sh} the flow rate of sheath fluid, $R_{Orifice}$ the inner diameter of O-pipette, η_{sa} the viscosity of sample fluid [20].

We have calculated the diameter of the microspheres from equations (1) and (2), and figure 3(*c*) shows both the experimental diameter of the droplet according to the change of the sheath flow rate (core and sample flow rates are fixed) and the calculated diameter under the same condition (both of the values are normalized, which means that both the experimental and the calculated diameters at a sheath flow rate of 6.0 mℓ h^{-1} were set to 1), and the results exhibit similar graph patterns. This outcome indicates that this analytical model is valid in our method (we use the aqueous solution instead of oil), and the size of the microcapsules can be predicted from this model. Figure 4(*a*) illustrates the produced microcapsule whose shell was solidified by its exposure to UV light: the dyed core fluid appears at the center, and these microcapsules mimic the eggs of frogs in nature. The cross-sectional scanning electron

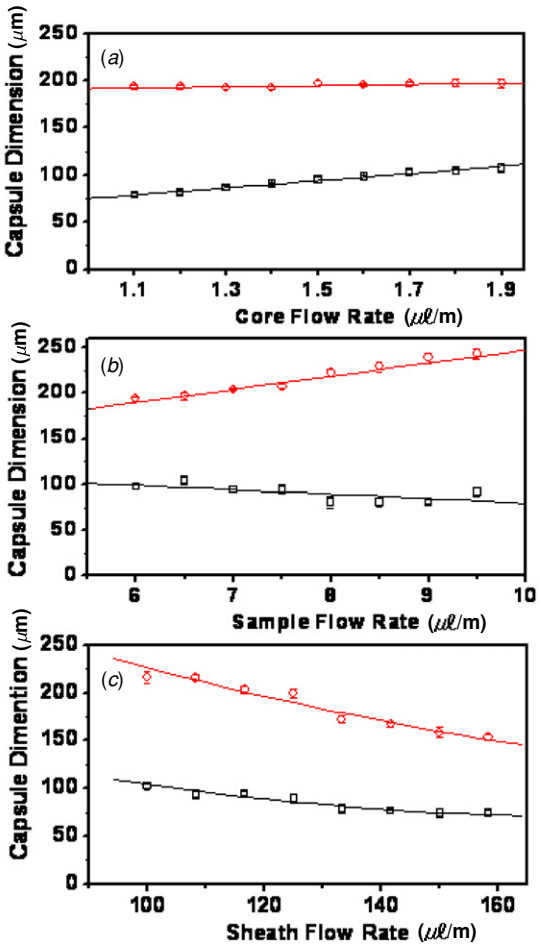

Figure 5. Variation of inner and outer diameters according to the change of (*a*) core flow rates: $Q_{sa} = 7.0\ \mu l\ min^{-1}$, $Q_{sh} = 133\ \mu l\ min^{-1}$, (*b*) sample flow rates: $Q_{co} = 1.85\ \mu l\ min^{-1}$, $Q_{sh} = 117\ \mu l\ min^{-1}$ and (*c*) sheath flow rates: $Q_{co} = 1.50\ \mu l\ min^{-1}$, $Q_{sa} = 7.0\ \mu l\ min^{-1}$ (lines are meant to guide the eye).

microscopy (SEM(S-4300, Hitachi)) image of the solidified microcapsule is illustrated in figure 4(*b*). The capsule was manually cut with the sharp razor under the stereoscopy, and some debris appear. The side view of the cut microcapsule is shown in the inset of figure 4(*b*), and the inner hole is clearly seen. We measured the size distribution of the microcapsules, and figure 4(*c*) illustrates the distribution of the inner and the outer diameters. The coefficients of variance (defined as the standard deviation divided by the diameter of the droplets) were about 4% and 5% for the inner and the outer diameters respectively, and these values are higher than that of Nie's results [19]. We conjectured that such a higher value resulted from our use of an aqueous solution as both sheath and core fluid.

We have measured the inner and the outer diameters according to the flow rate change of the core, sample and sheath fluid, and the results are plotted in figure 5. Figure 5(*a*) shows that the core fluid dominantly affects the determination of the microcapsule's inner diameter, while the outer diameter remains unaffected by the core flow rate. This finding indicates that the volume of loaded core fluid can be determined in reference to the core flow rates. As

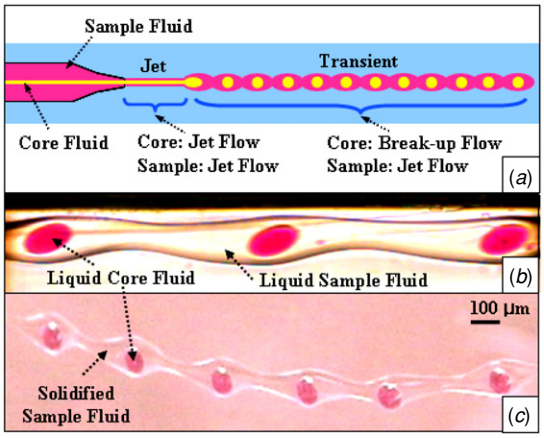

Figure 6. (*a*) Schematic illustration of transient flow generation. (*b*) Optical microscopy images of the transient flow: $Q_{co} = 1.25\ \mu l\ min^{-1}$, $Q_{sa} = 9.0\ \mu l\ min^{-1}$, $Q_{sh} = 133\ \mu l\ min^{-1}$. (*c*) Solidified transition flow (bundle of microcapsules) via UV exposure: $Q_{co} = 1.25\ \mu l\ min^{-1}$, $Q_{sa} = 8.0\ \mu l\ min^{-1}$, $Q_{sh} = 133\ \mu l\ min^{-1}$.

the sample flow rates increase, the inner diameter decreases, while the outer diameter increases, as demonstrated in figure 5(*b*). Therefore, the regulation of the sample fluid affects the thickness of the shell. As the flow rate of the sample fluid increases, the thickness of the shell increases. The sheath flow rate dominantly determines the outer diameter, as illustrated in figure 5(*c*). All these results involve the finding that the diversely sized microcapsules can be generated just by regulating the core, sample and sheath flow rates, respectively.

3.2. Fabrication of microcapsule bundle

Many researchers have focused on the production of single microcapsules, as described. However, we found that use of the same device can facilitate the production of bundles of microcapsules. Through a regulation of the flow rates of the core, sample and sheath fluids, the transient flow (outer: thread flow, inner: break-up (droplet) flow) as shown in figure 6(*a*) is generated. The mechanism of this transient flow is as follows: (1) the break-up of core fluid is formed inside the sample stream and (2) the jet thread of sample fluid is maintained inside the sheath stream. The range of the flow rates of the core, sample and sheath fluids in the generation of the transient flow is very narrow. Therefore, this state (transient flow) terminates by a small disturbance (e.g. vibration of a device or fluidic network). Figure 6(*b*) illustrates the transient flow formed inside the O-pipette, and the video image of the transient flow (outer: thread flow, inner: break-up) is demonstrated in M1 (at supporting material). We solidified this transient flow, and the micrograph of the solidified transient flow is demonstrated in figure 6(*c*), and its shape is a bundle of microcapsules. The mean volume per each capsule in the bundle was measured, its value being about 524 ± 20 picoliters. This result indicates that the production of bundled microcapsules is feasible just by the regulation of flow rates, and we expect that this bundle can be applied as a novel tool for the storing, handling and arrayed assay of such small volumes.

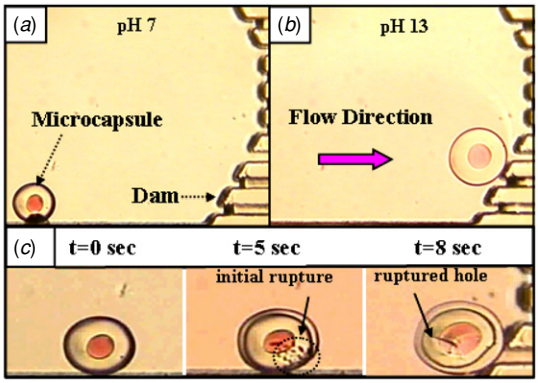

Figure 7. (*a*) Microcapsule in the microfluidic channel. The dam is used to prevent the capsule from moving out of the channel owing to the pressurized flow. (*b*) The swollen capsule by the base solution. The capsule is already ruptured. (*c*) The change of capsules at the appearance of the basic solution and according to the time track.

3.3. Controllable break of capsule

In terms of practical applications, there are two obstacles to be overcome. The first is how to break the microcapsule in a controllable way. Here, we added acrylic acid (AA) and EGDMA (cross-linker) to the sample fluid (solution 2 in table 1) for the controllable release of core fluid. The hydrogel polymerized with AA was employed as pH responsive components [31], and we fabricated microcapsules by using this solution. The produced pH responsive microcapsule was incorporated into the PDMS-based microfluidic channel (figure 7(*a*)), and the base (pH 13) solution was introduced into the channel (figure 7(*b*)). Then, the capsule rapidly swelled, as illustrated in figure 7(*c*), and the rupture took place within 10 s. This figure shows the rupturing process to the time track, and this relation indicates that the pH is one of the potential stimulating factors that break the microcapsule in a controllable way. As we view the matter, the controllable fracture of a microcapsule might constitute the critical challenge that future research will have to confront as it attempts to master the effective delivery of therapeutic materials in the treatment of disease.

3.4. Cell encapsulation

One advantage of this encapsulation method is that scientists can create the polymeric shell without attacking the target material (encapsulated core fluid). To verify this, we encapsulated yeast cells. Figure 8(*a*) shows the yeast cells and their fluorescent images. We detected the viability of cells by using a test kit (LIVE/DEAD® Yeast Viability Kit, Molecular Probes). The culture media containing stained yeast cells were employed as a core fluid. The microcapsules containing the yeast cells and their culture medium were fabricated and were stored for 2 days in non-aseptic water. The optical micrograph of these stored microcapsules and their corresponding fluorescent micrograph are illustrated in figure 8(*b*), and the cells were still alive. These results indicate that, owing to the polymeric shell, the cells can escape not only from attacks during the fabrication process but also from the harsh environment and from infections; consequently, there

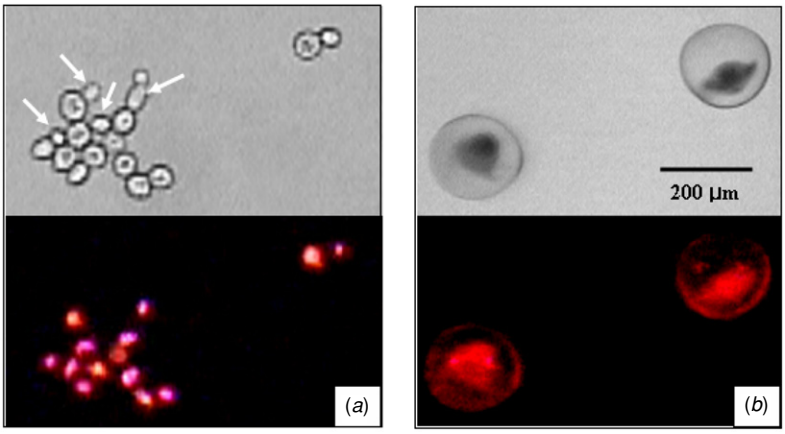

Figure 8. (*a*) Stained cells and their corresponding fluorescent image. Dead cells (indicated by arrows) do not appear in the fluorescent image. (*b*) Encapsulated live cells after 2 days storage in the non-aseptic water.

is, herein, a potential application of cell delivery to specific regions.

4. Conclusion

In conclusion, we have developed a simple and cost effective method for the fabrication of microcapsules that encapsulate materials in a liquid state by means of hydrodynamic phenomena and *in situ* photopolymerization, and the flexibility of the method across both different materials and different scales is a key advantage. As the fabrication is carried out without any kinds of physical and chemical attacks, even very sensitive materials can be loaded into the capsule without any damage. The shells can protect the target materials from the harsh environment, a conclusion that we inferred from the yeast cell culture experiment. The suggested technology can be applied extensively to the delivery and the storage of sensitive materials—materials that are being isolated in surrounding environments. We expect that possible applications will include combinatorial cell assays, FACS-like assays, the production of artificial eggs and polymer encapsulation for cell-based therapies.

Acknowledgment

This study was supported by a grant from the Korea Health 21 R&D Project, Ministry of Health & Welfare, Republic of Korea (0405-ER01-0304-0001).

References

[1] Yeo Y and Park K 2004 A new microencapsulation method using an ultrasonic atomizer based on interfacial solvent exchange *J. Control. Release* **100** 379–88
[2] Meng F, Engbers G H M and Feijen J 2005 Biodegradable polymersomes as a basis for artificial cells: encapsulation, release and targeting *J. Control. Release* **101** 187–98
[3] Berkland C, Pollauf E, Pack D W and Kim K 2004 Uniform double-walled polymer microspheres of controllable shell thickness *J. Control. Release* **96** 101–11
[4] Loscertales I G, Barrero A, Guerrero I, Cortijo R, Marquez M and Ganan-Calvo A M 2002 Micro/nano encapsulation via electrified coaxial liquid jets *Science* **295** 1695–8
[5] Orive G *et al* 2003 Cell encapsulation: promise and progress *Nature Med.* **9** 104–7
[6] Peyratout C S and Daehne L 2004 Tailor-made polyelectrolyte microcapsules: from multilayers to smart containers *Angew. Chem. Int. Ed.* **43** 3762–83
[7] Liu R, Ma G H, Meng F and Su Z 2005 Preparation of uniform-sized PLA microcapsules by combining Shirasu Porous Glass membrane emulsification technique and multiple emulsion-solvent evaporation method *J. Control. Release* **103** 31–43
[8] Pekarek K J, Jacob J S and Mathlowitz E 1994 Double-walled polymer microspheres for controlled drug release *Nature* **367** 258–60
[9] Song H, Tice J D and Ismagilov R F 2003 A microfluidic system for controlling reaction networks in time *Angew. Chem. Int. Ed.* **42** 768–72
[10] Thorsen T, Roberts R W, Arnold F H and Quake S R 2001 Dynamic pattern formation in a vesicle-generating microfluidic device *Phys. Rev. Lett.* **86** 4163–6
[11] Tan Y C, Fisher J S, Lee A I, Cristini V and Lee A P 2004 Design of microfluidic channel geometries for the control of droplet volume, chemical concentration, and sorting *Lab Chip* **4** 292–8
[12] Nisisako T, Torii T and Higuchi T 2002 Droplet formation in a microchannel network *Lab Chip* **2** 24–6
[13] Tice J D, Song H, Lyon A D and Ismagilov R F 2003 Formation of droplets and mixing in multiphase microfluidics at low values of the Reynolds and the capillary numbers *Langmuir* **19** 9127–33
[14] Okushima S, Nisisako T, Torii T and Higuchi T 2004 Controlled production of monodisperse double emulsions by two-step droplet breakup in microfluidic devices *Langmuir* **20** 9905–8
[15] Zheng B, Tice J D and Ismagilov R F 2004 Formation of arrayed droplets by soft lithography and two-phase fluid flow, and application in protein crystallization *Adv. Mater.* **16** 1365–8
[16] Jeong W J, Kim J Y, Kim S J, Lee S H, Mensing G and Beebe D J 2004 Hydrodynamic microfabrication via 'on the fly' photopolymerization of microscale fibers and tubes *Lab Chip* **4** 576–80
[17] Jeong W J, Kim J Y, Choo J, Lee E K, Han C S, Beebe D J, Seong G H and Lee S H 2005 Continuous fabrication of biocatalyst immobilized microparticles using photopolymerization and immiscible liquids in microfluidic systems *Langmuir* **21** 3738–41
[18] Xu S, Nie Z, Seo M, Lewis P, Kumacheva E, Stone H A, Garstecki P, Weibel D B, Gitlin I and Whitesides G M 2005 Generation of monodisperse particles by using

microfluidics: control over size, shape, and composition *Angew. Chem. Int. Ed.* **117** 734–8
[19] Nie Z, Xu S, Seo M, Lewis P C and Kumacheva E 2005 Polymer particles with various shapes and morphologies produced in continuous microfluidic reactors *J. Am. Chem. Soc.* **127** 8058–63
[20] Utada A S, Lorenceau E, Link D R, Kaplan P D, Stone H A and Weitz D A 2005 Monodisperse double emulsions generated from a microcapillary device *Science* **308** 537–41
[21] Schneeweiss I and Rehage H 2005 Non-spherical capsules for food industry *Chem. Ing. Tech.* **77** 236–9
[22] Rayleigh L 1879 On the capillary phenomena of jets *Proc. R. Soc.* **29** 71–97
[23] Cristini V and Tan Y C 2004 Theory and numerical simulation of droplet dynamics in complex flows—a review *Lab Chip* **4** 257–64
[24] Link D R, Anna S L, Weitz D A and Stone H A 2004 Geometrically mediated breakup of drops in microfluidic devices *Phys. Rev. Lett.* **92** 054503(1–4)
[25] Anna S L, Bontoux N and Stone H A 2003 Formation of dispersions using 'flow focusing' in microchannels *Appl. Phys. Lett.* **82** 364–66
[26] Cristini V, Guido S, Alfani A, Blawzdziewics J and Loewenberg M 2003 Drop breakup and fragment size distribution in shear flow *J. Rheol.* **47** 1283–98
[27] Lin S P and Leitz R D 1998 Drop and spray formation from a liquid jet *Annu. Rev. Fluid Mech.* **30** 85–105
[28] Coulliette C and Pozrikids C 1998 Motion of an array of drops through a cylindrical tube *J. Fluid Mech.* **358** 1–28
[29] Cramer C, Beruter B, Fischer P and Windhab E J 2002 Liquid jet stability in a laminar flow field *Chem. Eng. Technol.* **25** 499–506
[30] Ambravaneswaran B, Subramani H J, Phillips S D and Basaran O A 2004 Dripping-jetting transitions in a dripping faucet *Phys. Rev. Lett.* **93** 034501(1–4)
[31] Beebe D J, Moore J S, Bauer J M, Yu Q, Liu R H, Devadoss C and Jo B H 2000 Functional hydrogel structures for autonomous flow control inside microfluidic channels *Nature* **404** 588–90